Discovery of Tyrosinase Inhibitors: Structure-Based Virtual Screening and Biological Evaluation

Guan Wang[1,#] Jin Li[1,#] Xiao-Li Pan[1] Fa-Qian Bu[1] Yu-Meng Zhu[1] Ao-Xue Wang[1] Liang Ouyang[1*]

[1] State Key Laboratory of Biotherapy and Cancer Center, Innovation Center of Nursing Research, Nursing Key Laboratory of Sichuan Province, West China Hospital, Sichuan University, Chengdu, People's Republic of China

Address for correspondence Liang Ouyang, PhD, State Key Laboratory of Biotherapy and Cancer Center, Innovation Center of Nursing Research, Nursing Key Laboratory of Sichuan Province, West China Hospital, Sichuan University, Chengdu 610041, People's Republic of China (e-mail: ouyangliang@scu.edu.cn).

Pharmaceut Fronts 2022;4:e1–e8.

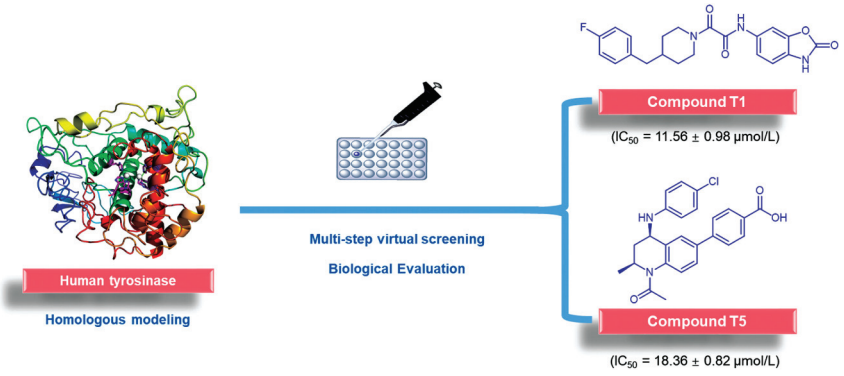

Abstract

Tyrosinase (EC 1.14.18.1) plays an indispensable role in the rate-limiting steps of melanin biosynthesis, and its uncontrolled activity may result in various diseases, such as albinism, melanoma, freckles, etc. The inhibition of tyrosinase activity may provide a useful and efficient strategy to treat hyperpigmentation disorders. However, the widely used tyrosinase inhibitors, like α-arbutin, hydroquinone, and kojic acid, have many shortcomings, such as lower efficacy and much more side effects. Herein, we reported the use of homology modeling and multistep structure-based virtual screening for the discovery of novel tyrosinase inhibitors. In this study, 10 initial potential hits (compounds **T1–T10**) were evaluated for enzyme inhibition and kinetic study, with kojic acid being used as a control. Among them, the IC_{50} values of both **T1** (11.56 ± 0.98 μmol/L) and **T5** (18.36 ± 0.82 μmol/L) were superior to that of kojic acid (23.12 ± 1.26 μmol/L). Moreover, **T1** and **T5** were also identified as the effective noncompetitive tyrosinase inhibitors by the subsequent kinetic study. Above all, **T1** and **T5** may represent the promising drug candidates for hyperpigmentation therapy in pharmaceutical fields, as well as the effective whitening agents in cosmetic applications.

Keywords

- tyrosinase inhibitors
- hyperpigmentation
- homology modeling
- virtual screening
- kinetic study

[#] *These authors contributed equally to this work.*

received
October 21, 2021
accepted
December 7, 2021

DOI https://doi.org/10.1055/s-0041-1742095.
ISSN 2628-5088.

Georg Thieme Verlag KG, Rüdigerstraße 14, 70469 Stuttgart, Germany

Introduction

Tyrosinase (EC 1.14.18.1) is a type III metalloprotease and oxidoreductase containing two copper ions in the active center accompanied by six histidine residues. Tyrosinase is widespread in microorganisms, plants, animals, and humans, and plays the key role as the rate-limiting enzyme in melanin biosynthesis.[1] Melanin contributes to cuticular hardening and exoskeletal pigmentation in animals, and enzymatic browning in fruits and vegetables.[2,3] And the color of human skin is predominantly determined by the amount of melanin produced by skin melanocytes. Melanin can prevent the skin from the side effects of environmental factors such as ultraviolet radiation and oxidative stress. However, excessive accumulation of melanin results in pigmentation diseases including freckles, age spots, melanosis, malignant melanoma, etc.[4] In this case, tyrosinase inhibitors, such as kojic acid, α-arbutin, hydroquinone, and azelaic acid, are considered as important skin-whitening agents or food preservatives in the fields of medicine, cosmetics, and food. However, they have certain side effects and cannot be widely used.[5] Thus, developing novel efficient and selective inhibitors for tyrosinase remained significantly important.

Computer-aided drug design (CADD) represents an effective tool for drug discovery, which can largely reduce the cost of drug discovery and increase the feasibility of drug screening. It is acknowledged that virtual screening of molecular docking based on receptor structure is a common method in drug design.[6] Virtual screening from a large database is based on the three-dimensional (3D) structure of receptor enzymes to discover novel ligands.[7] The binding affinity of ligand–receptor complexes can be predicted according to the interaction between ligands and protein macromolecules, thus favoring the discovery of a better ligand structure.[8] Obviously, computer technology can simulate a more real binding state of ligand and receptor, greatly reducing the number of the wet-lab ligand activity experiments and saving a lot of manpower, material, and financial resources.[9] However, virtual screening based on receptor structure is often dominated by visual inspection of medicinal chemists in the later stage,[10] and many target proteins are still short of a clear and complete crystal structure, which together greatly limit the wide application of the tool.[11]

Herein, we reported a multiple-step virtual screening method of receptor structure, based on the homologous modeling of human tyrosinase. Potential active molecules were selected from the compound library constructed by our laboratory for tyrosinase biological activity test. In our study, two noncompetitive tyrosinase inhibitors (**T1** and **T5**) with novel skeleton structures were obtained. Compounds **T1** and **T5** may be used as promising drug candidates for hyperpigmentation treatment, and whitening agents in cosmetic applications.

Results and Discussion

Homologous Modeling Results

Human tyrosinase belongs to a family of transmembrane glycoproteins and faces a lot of challenges toward stable crystallization at a high concentration.[12] Until now, there is still no available cocrystal structure of human tyrosinase. A homology modeling strategy shrinks the gap between the amino sequence and the 3D structure of protein.[13] In this study, a homology modeling was performed using the Swiss-model for the virtual screening.[14] First, an amino acid sequence of human tyrosinase (P14679) was retrieved in the UniProt database.[15] After importing the amino acid sequence, the results showed that the template system selected was human tyrosinase-related protein 1 (TYRP-1) (PDB ID: 5M8L), which had four chains A, B, C, and D and was the crystal structure of TYRP-1 and 2-acetamido-2-deoxy-β-*D*-glucopyranose.[16] A chain was chosen by the system automatically. The total length of the chain sequence was 446, and the resolution was 2.35 Å. The homologous modeling of human tyrosinase was established by the Swiss-model. The sequence identity between human tyrosinase and TYRP-1 was 43.32% and the global model quality estimate value was 0.67. The amino acid residues of the homologous modeling were from His19 to Gln453, the total sequence length was 435, and both Met1-Glu18 and Asp454-Leu529 were missing. The active site of human tyrosinase was similar to that of mushroom tyrosinase (PDB ID: 2Y9X), which contained two metal ions coordinated with six histidine residues.[17] On the basis of the mentioned protein preparation work above, we conducted the multiple-step virtual screening targeting tyrosinase.

Structure-Based Virtual Screening

Molecular docking plays a common and important role in the area of structural molecular biology and CADD. There are numerous successful examples obtained with the help of this method.[18] Molecular docking can speed up the pace of drug development and lower down the costs. ►**Fig. 1** shows the process of a multiple-step virtual screening in discovering lead inhibitors of human tyrosinase. In the first turn, small-molecule compound databases including SPECS, ACDB, and MCDB with more than 200,000 compounds were filtered by the Lipinski's rule of five.[19] It is well known that the molecule with the following features would be more likely to result in a real small-molecule drug: (1) a molecular mass less than 500 Da; (2) no more than 10 hydrogen bond acceptors; (3) no more than five hydrogen bond donors; and (4) log *P* (octanol–water partition coefficient) no greater than 5.[20] In addition, all of these compounds are commercially available or synthesized in laboratory, and could be picked out for further biological evaluation. In this study, a total of 198,460 small-molecule compounds were obtained for the following docking-based virtual screening.

Next, the filtered databases were screened by molecular docking using the crystal structure of human tyrosinase in the HTVS (high-throughput virtual screening) module of Glide. The top 5,000 hits with a Glide docking score ranging from −7.97 to −3.52 kcal/mol were screened. Afterward, the 5,000 hits were docked precisely with human tyrosinase in the SP (standard precision) module of Glide. The top 150 candidates were selected for the docking pattern analysis, whose Glide docking scores were greater than −4.12

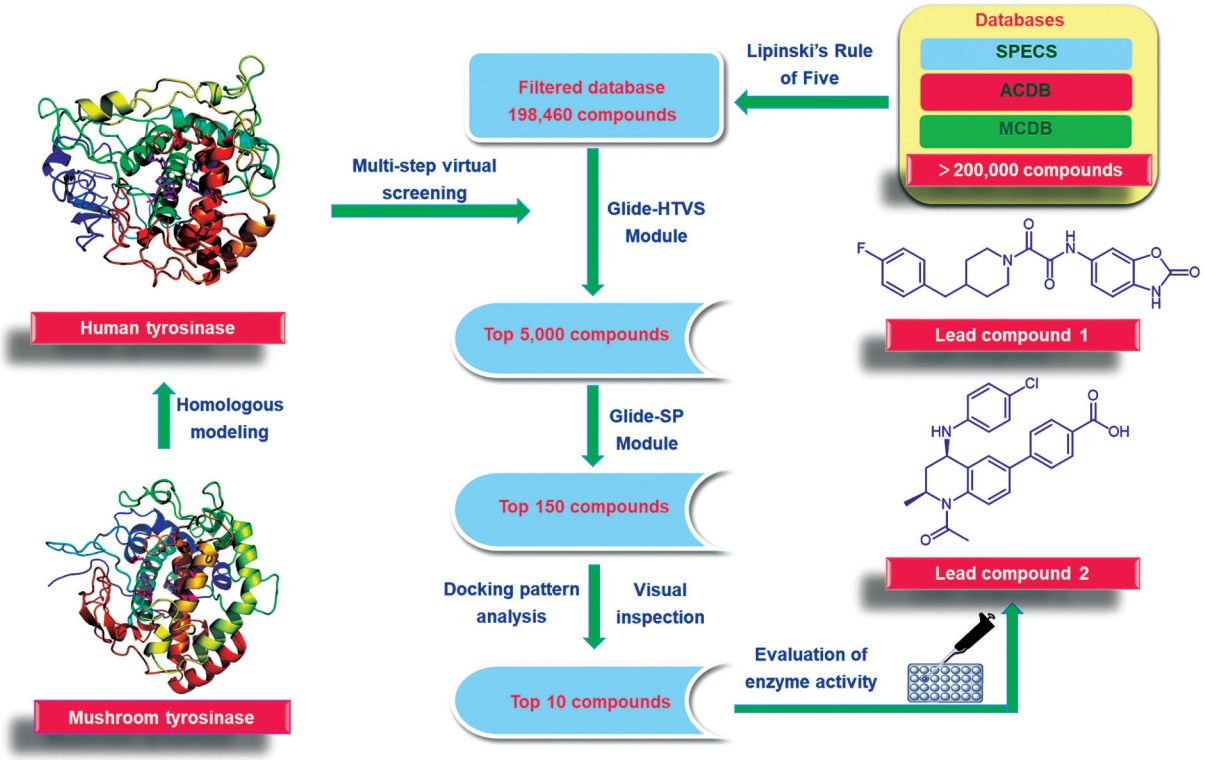

Fig. 1 The workflow of discovering tyrosinase inhibitors based on a multistep structure-based virtual screening.

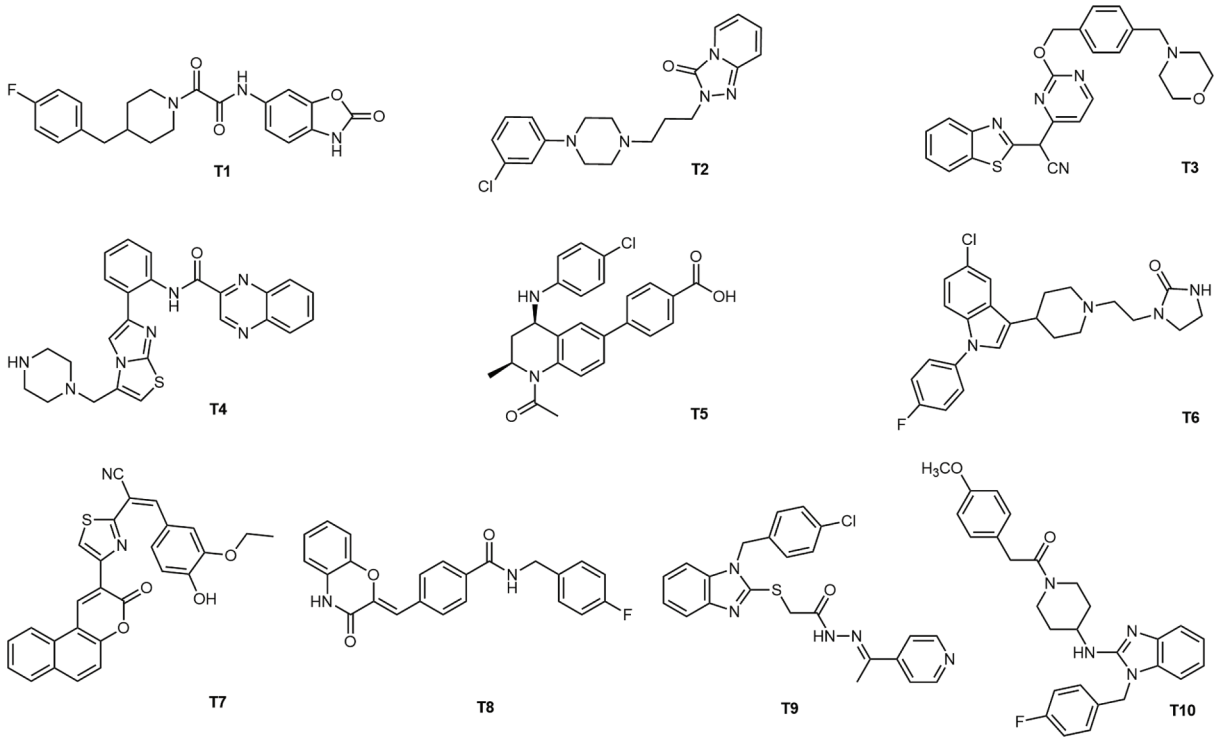

Fig. 2 The chemical structures of 10 lead hits prepared for the biological activity assays.

kcal/mol. We searched the professional advice of pharmaceutical chemists to classify the 150 candidates by visual inspection according to their structural features. In this process, the docking score, the interaction between key amino acids and ligands, the match degree of compound conformation and protein, the interaction patterns, and especially the novelty of molecular skeleton were highly considered.[21] Consequently, the 10 hits with different skeletons were purchased from SPECS database and determined for the following tyrosinase inhibition assay (►**Fig. 2**).

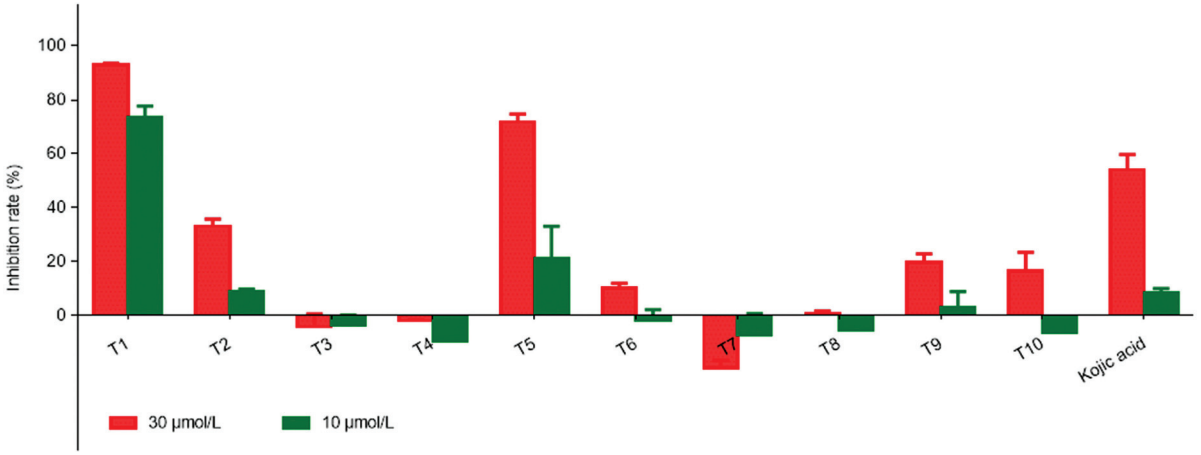

Fig. 3 The preliminary screening results of mushroom tyrosinase inhibitory activity of 10 lead hits performed at 10 and 30 μmol/L using *L*-tyrosine as the substrate. Data are presented as means ($n = 3$).

Mushroom Tyrosinase Inhibition Assay

To carry out the tyrosinase inhibition assay, mushroom tyrosinase was used to detect the inhibition rate of 10 hits. Mushroom tyrosinase is commercially available, highly homologous to mammalian enzyme in the active center, and is one of the most common tyrosinase enzymes used today.[4] Kojic acid is a well-known whitening agent in cosmetic field and a food additive in preventing enzymatic browning. Kojic acid inhibits tyrosinase activity, and was used as a positive control in the biological activity assay according to a reported study.[22] The results of the preliminary screening of tyrosinase inhibitory activity (►**Fig. 3**) showed that four hits (compounds **T3**, **T4**, **T7**, and **T8**) exerted no inhibitory potency at two concentrations. Four hits (compounds **T2**, **T6**, **T9**, and **T10**) showed moderate inhibitory activity at the concentration of 30 μmol/L. Obviously, compounds **T1** and **T5** exhibited stronger tyrosinase inhibitory potency than the positive control kojic acid. Tyrosinase inhibition rates of **T1** and **T5** were 90 and 70%, respectively, at the concentration of 30 μmol/L, while over 70 and 20%, respectively, at the concentration of 10 μmol/L. Thus, **T1** and **T5** were chosen for the further IC_{50} (half-maximal inhibitory concentration) measurement.

IC_{50} is a measure of the effectiveness of inhibitors in medicinal chemistry.[23] IC_{50} is defined as the concentration of an inhibitor that inhibits up to 50% in such biosystem like enzyme. Then, a dose–response curve for **T1** and **T5** was constructed using GraphPad Prism 6 (version 6.01). The results showed that **T1** and **T5** dose-dependently inhibited the tyrosinase activity (►**Fig. 4A**). And the IC_{50} values of **T1** and **T5** were 1.56 ± 0.98 and 18.36 ± 0.82 μmol/L, respectively, much lower than that of kojic acid (23.12 ± 1.26 μmol/L). Particularly, compound **T1** exhibited the best inhibitory activity with more than twofold inhibitory potency in comparison to the control. In short, compounds **T1** and **T5** were effective tyrosinase inhibitors, and their inhibition mechanisms were further explored in the following study.

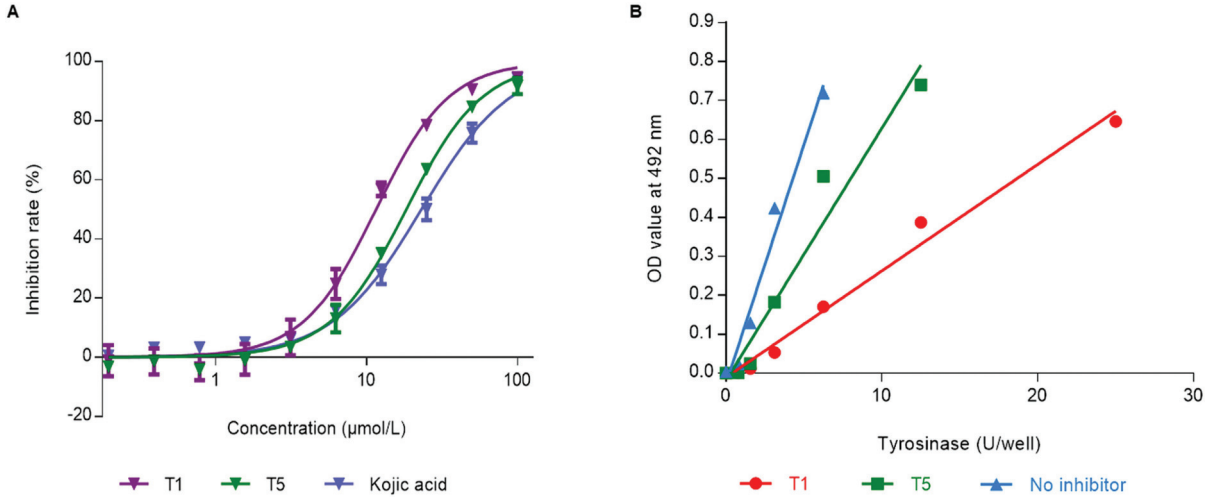

Fig. 4 Inhibition effect and inhibition mechanism assays of **T1** and **T5**. (**A**) Inhibition rate curve against mushroom tyrosinase inhibitory. (**B**) Determining inhibition type for mushroom tyrosinase activity. Each experiment was repeated in three parallels.

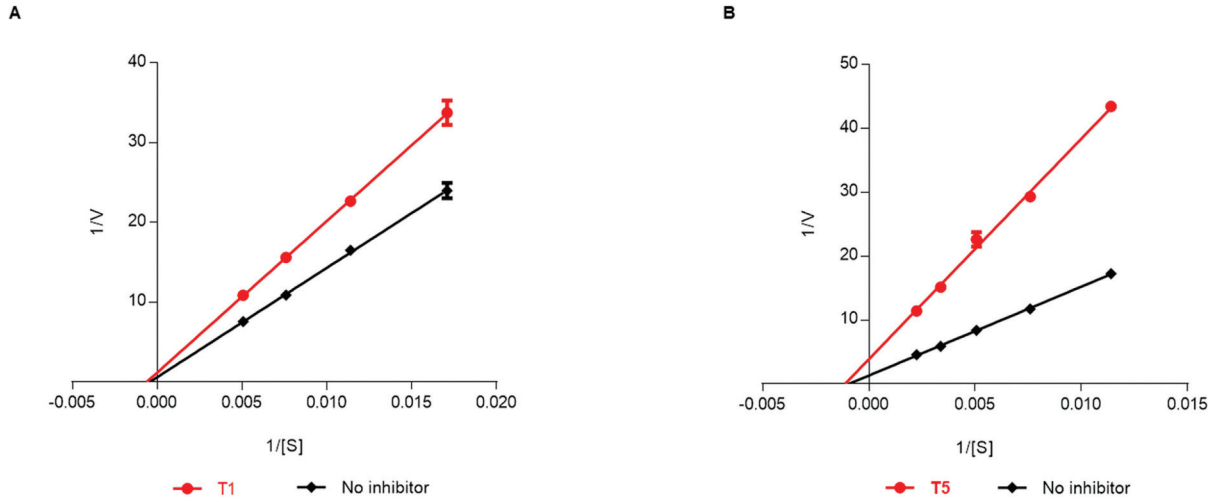

Fig. 5 Lineweaver–Burk double-reciprocal plot of (**A**) **T1** and (**B**) **T5** upon mushroom tyrosinase inhibitory. Results were acquired including mean values of 1/*V*, which was the inverse of the increasing value of the absorbance at the 492 nm wavelength per minute with different concentrations of *L*-tyrosine being used as the substrate. All experiments were performed in triplicate, and data were presented as means ± SEM. SEM, standard error of the mean.

Kinetic Study of Tyrosinase Inhibition

To identify the inhibition type of two lead hits, the relationship between substrate concentration and enzymatic reaction rate was illustrated by the GraphPad Prism 6 (version 6.01). An inhibitor was determined to be irreversible or reversible according to whether the two lines were parallel or intersected at origin. ►**Fig. 4B** shows that the three lines intersected at origin. **T1** and **T5** decreased the slope of the straight line, inhibited the enzyme activity, and led to the reduction in the catalytic efficiency of tyrosinase (instead of through reducing the effective enzyme amount). All above results suggested that **T1** and **T5** were reversible tyrosinase inhibitors.

Furthermore, the reaction rates of the lead hit with different concentrations of *L*-tyrosine were also collected, and a Lineweaver–Burk double-reciprocal plot was analyzed to evaluate the inhibition type of the two lead hits in depth. The kinetic study showed that both the curves of **T1** and **T5** intersected on the *X*-axis (►**Fig. 5**), indicating that **T1** and **T5** were noncompetitive inhibitors of mushroom tyrosinase due to the decreased V_{max} value and the unchanged K_m (the Michaelis constant) value. Moreover, for each lead hit, the K_i (the inhibitory constant) value was also calculated from the plot.[24] The K_i value of **T1** and **T5** was 11.35 and 17.7 μmol/L, respectively, indicating that in comparison to **T5**, **T1** had a higher affinity with mushroom tyrosinase, which was consistent with the results from IC_{50} assay (►**Table 1**).

Molecular Docking Results

Then molecular docking analyses of **T1** and **T5** in silicon were performed using the protocol of Ligand Interaction Diagram of SchrödingerSuite and Protein–Ligand Interaction Profiler (PLIP). Our data suggested that **T1** and **T5** had a similar binding mode and site to human tyrosinase. ►**Fig. 6A** shows the docking results of **T1**, which shows that the ligand molecule was stabilized by intermolecular hydrogen bonds with Asp197, Glu203, and Gln378, and π–π stacking interactions with His367. In addition, the fluorine atom was oriented toward the metal ions in the active center and formed a halogen bond with Ser380, which was beneficial to stable the complex of the ligand and human tyrosinase. The ligand molecule could interact with the surrounding amino residues, including Phe347, His367, Ile368, and Val377, through the hydrophobic contact. ►**Fig. 6B** shows the docking results of **T5**, which displays that the carboxyl group could chelate with the metal ion in the active center, and the benzene ring might form π–π interaction with His202 and His367. The chlorine atom can interact with Gln378 through halogen interaction, while the benzylpiperidine moiety formed π–π interaction with Phe347. In addition, the ligand formed hydrogen bonds with

Table 1 Mushroom tyrosinase inhibitory activity and kinetic assays of two lead hits

Compound	IC_{50} (μmol/L)[a]	K_i (μmol/L)[b]	Type of inhibition	Docking score (kcal/mol)[c]
T1	11.56 ± 0.98	11.35	Noncompetitive	−5.576
T5	18.36 ± 0.82	17.7	Noncompetitive	−6.920
Kojic acid	23.12 ± 1.26	–	–	−4.996

[a]Data are presented as means ± SEM from three parallels.
[b]K_i values were obtained at the concentration of 30 μmol/L of **T1** and **T5**.
[c]Docking scores were collected from SP module of Glide docking.

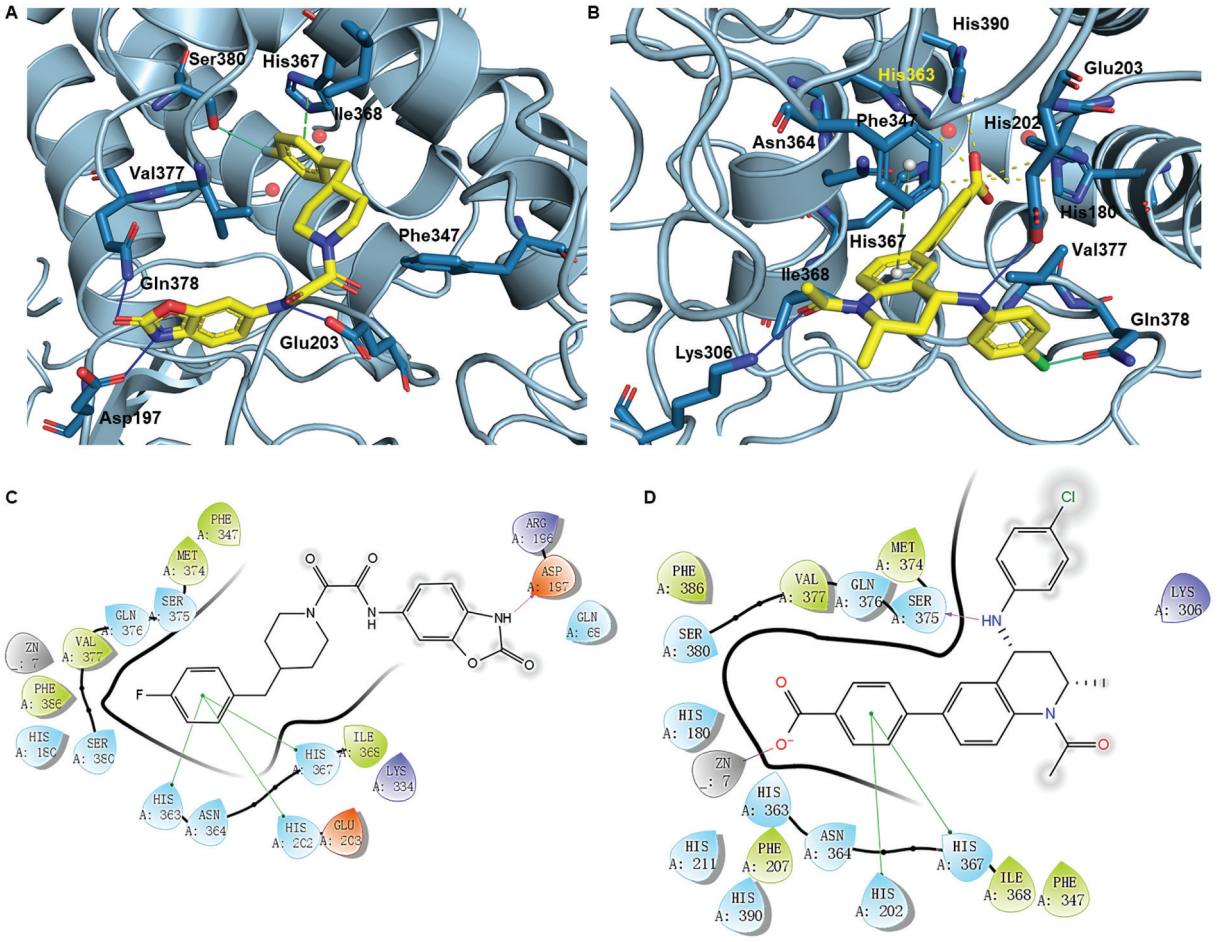

Fig. 6 Docking results of compound (**A**) **T1** and (**B**) **T5** in the active center of human tyrosinase, as well as the 2D interaction pattern of human tyrosinase with (**C**) **T1** and (**D**) **T5**. Analysis of human tyrosinase bearing the active center was performed by the cartoon model. The active center contained two metal ions shown as *red spheres* accompanied by key residues (*light blue* stands for carbon; *bright blue* stands for nitrogen; *red* stands for oxygen) displayed in the stick model. The ligand is shown in the stick model (*yellow* stands for carbon; *blue* stands for nitrogen; *red* stands for oxygen; *green* stands for halogen). 2D, two-dimensional.

Ser375 and Lys306, as well as hydrophobic interactions with Asn364, His367, Ile368, and Val377, making the complex more stable. The two-dimensional interaction patterns between **T1** and human tyrosinase (►**Fig. 6C**) and **T5** and human tyrosinase (►**Fig. 6D**) are also illustrated. Our data showed that the docking scores of **T1** (−5.576 kcal/mol) and **T5** (−6.920 kcal/mol) were much higher than that of the control (−4.996 kcal/mol) with the optimal docking results being seen in **T5** (►**Table 1**). Thus, we predicted that the chelation of carboxyl group and metal ion in the active site might be the main factor affecting the docking results. The interaction with metal ions or histidine residues in the active center might directly enhance the inhibitory effect on tyrosinase.

Conclusion

In summary, we have introduced a multistep virtual screening process using CADD methods including molecular docking and homology modeling. Compounds **T1** and **T5**, along with other eight potential active compounds, were picked out through virtual screening from the database containing more than 200,000 small-molecule compounds. Excitedly, **T1** and **T5** were identified as effective noncompetitive reversible tyrosinase inhibitors. The IC_{50} values of the two inhibitors were 11.56 ± 0.98 and 18.36 ± 0.82 μmol/L, respectively, which were superior to the positive drug kojic acid (23.12 ± 1.26 μmol/L). Our experimental results provided a strong basis for the efficiency of our screening and docking strategies. Our study enriched the function study of human tyrosinase, suggested two promising drug candidates (**T1** and **T5**) for the treatment of hyperpigmentation and malignant melanoma, and provided two potential whitening agents for the cosmetic field. Furthermore, the appropriate structure optimization of **T1** and **T5** and structure–activity relationship study need to be further studied in our laboratory; unfortunately, data are unavailable at present.

Methods and Materials

Homology Modeling

Homology modeling was performed according to previous studies.[25] The 3D structure of human tyrosinase protein was simulated by the Swiss-model.[26] The amino acid sequence of human tyrosinase was downloaded from the UniProt

database (https://www.uniprot.org/; ID: P14679).[27] The sequence was copied to the Swiss-model Target Sequence and the project request was submitted. The server returned the homology modeling result after a period of time.

Structure-Based Virtual Screening

Protein Preparation

Homology modeling was used to construct the 3D structure of human tyrosinase. Human tyrosinase was optimized using the Protein Preparation Wizard module of Maestro (version 11.8) in SchrödingerSuite (Schrödinger, LLC, New York, NY, United States) with default parameters to remove water molecules, add hydrogen atoms, and fill in missing residues.[28] The active site was defined in the active site containing metal ions through the Receptor Grid Generation module.

Database Preparation

The databases including SPECS, ACDB, and MCDB were filtered in accordance with Lipinski's rule of five. The structures of all molecules were optimized by the LigPrep module with the OPLS_2005 force field being in an ionized state at pH 7.0 ± 2.0, and the default parameters being used to generate the 3D structure.[29] The optimized database was saved as Maestro file format.

Molecular Docking

Molecular docking of human tyrosinase was performed by the Ligand Docking module. The protein structure was derived from homology modeling. First, the Glide module HTVS was used to roughly evaluate the binding affinity of the human tyrosinase and the ligands in the prepared database in the active site.[30] Then, the top 5,000 hits were selected and docked precisely with human tyrosinase by SP and XP (Extra Precision) modules, leaving the top 150 leads.[31] Analysis and visualization of the molecular docking results were completed by means of Ligand Interaction Diagram and PLIP tool.[32]

Mushroom Tyrosinase Inhibition Assay

The enzyme inhibitory activity assay was performed according to previous studies.[33,34] In brief, a total of 0.1 mL reaction system was added to a 0.5 mL centrifuge tube, which contained 50 μL sample (10 and 30 μmol/L, respectively) and mushroom tyrosinase (25 μL, 1 mmol/L). The mixed solution was maintained at 25°C for 20 minutes, and then *L*-tyrosine (25 μL, 2.5 U/μL) as a substrate was added quickly and mixed well. The change of optical density (OD) value was measured within 5 minutes at 492 nm. DMSO-containing phosphate buffer (50 μL) was used as a vehicle control plate, while DMSO-containing phosphate buffer (75 μL) and *L*-tyrosine (25 μL, 2.5 U/μL) was used as a blank control plate. The inhibition rate was calculated with the following Eq. (1).

$$\text{Inhibition rate}\,(\%) = \frac{\Delta OD_{\text{vehicle}} - \Delta OD_{\text{compound}}}{\Delta OD_{\text{vehicle}} - \Delta OD_{\text{blank}}} \times 100\% \quad (1)$$

where $\Delta OD_{\text{compound}}$ is the changed OD value after inhibitor treatment, $\Delta OD_{\text{vehicle}}$ is the OD value for the vehicle control plate, and ΔOD_{blank} is the OD value for the blank control.

IC_{50} Assay

IC_{50} assays for **T1** and **T5** were further assessed. Different concentrations (less than 1 mmol/L) of **T1** and **T5** were dissolved in DMSO, respectively. The changed OD value for each solution in the 0.1 mL reaction system was measured according to the method under the heading "Mushroom Tyrosinase Inhibition Assay." The tyrosinase activity rate was calculated according to the inhibition rate of Eq. (1). The dose–response curve was drawn by GraphPad Prism 6 (version 6.01). The IC_{50} value for each compound was obtained according to the dose–response curve.

Kinetic Study

The kinetic study was performed according to a reported study.[35] We prepared 30 μmol/L of **T1** and **T5**, and different concentrations of mushroom tyrosinase (0.78, 1.56, 3.125, 6.25, 12.5, 25, 50, and 100 U/well). The enzyme catalytic activity was evaluated using the method under the heading "Mushroom Tyrosinase Inhibition Assay." The blank control was investigated in the same dose except for the addition of inhibitors. The curves were made by GraphPad Prism 6 (version 6.01) to illustrate the relationship between tyrosinase concentration and the tyrosinase enzyme activity.

The inhibition mechanisms of **T1** and **T5** were further studied. *L*-tyrosine was prepared at the concentration of 1,000, 667, 444, 296, 198, 132, 88, 59, and 39 nmol/L, respectively. The blank control was performed in the same dose except for the addition of inhibitors. The catalytic activity of tyrosinase enzyme was completed respectively according to the method under the heading "Mushroom Tyrosinase Inhibition Assay." Lineweaver–Burk double-reciprocal plots were determined by the reciprocal $1/[S]$ (the concentration of *L*-tyrosine), the reciprocal $1/V$ (the enzyme catalytic activity for OD change), and the K_m, and maximum velocity (V_{max}) values were calculated later.[36]

Funding

This work was supported by the National Natural Science Foundation of China (Grant No. 81922064, 22177083, 81803755, and 81874290).

Conflict of Interest

All authors declare no conflict of interest.

References

1 Li J, Feng L, Liu L, et al. Recent advances in the design and discovery of synthetic tyrosinase inhibitors. Eur J Med Chem 2021; 224:113744
2 Friedman M. Food browning and its prevention: an overview. J Agric Food Chem 1996;44:631–653
3 Kramer KJ, Hopkins TL. Tyrosine metabolism for insect cuticle tanning. Arch Insect Biochem Physiol 1987;6:279–301
4 Pillaiyar T, Namasivayam V, Manickam M, Jung SH. Inhibitors of melanogenesis: an updated review. J Med Chem 2018;61(17): 7395–7418
5 Boo YC. Human skin lightening efficacy of resveratrol and its analogs: from in vitro studies to cosmetic applications. Antioxidants 2019;8(09):332

6 Basak SC, Vracko M, Bhattacharjee AK. Big data and new drug discovery: tackling "Big Data" for virtual screening of large compound databases. Curr Comput Aided Drug Des 2015;11 (03):197–201
7 Lyu J, Wang S, Balius TE, et al. Ultra-large library docking for discovering new chemotypes. Nature 2019;566(7743):224–229
8 Mysinger MM, Shoichet BK. Rapid context-dependent ligand desolvation in molecular docking. J Chem Inf Model 2010;50 (09):1561–1573
9 Ferreira LG, Dos Santos RN, Oliva G, Andricopulo AD. Molecular docking and structure-based drug design strategies. Molecules 2015;20(07):13384–13421
10 Waszkowycz B. Towards improving compound selection in structure-based virtual screening. Drug Discov Today 2008;13(5–6):219–226
11 Rondeau JM, Schreuder H. Chapter 22 - Protein crystallography and drug discovery. In: Wermuth CG, Aldous D, Raboisson P, et al., eds. The Practice of Medicinal Chemistry. 4th ed. San Diego: Academic Press; 2015:511–537
12 Mendes E, Perry MdeJ, Francisco AP. Design and discovery of mushroom tyrosinase inhibitors and their therapeutic applications. Expert Opin Drug Discov 2014;9(05):533–554
13 Waterhouse A, Bertoni M, Bienert S, et al. SWISS-MODEL: homology modelling of protein structures and complexes. Nucleic Acids Res 2018;46(W1):W296–W303
14 Studer G, Rempfer C, Waterhouse AM, Gumienny R, Haas J, Schwede T. QMEANDisCo-distance constraints applied on model quality estimation. Bioinformatics 2020;36(06):1765–1771
15 UniProt Consortium. UniProt: the universal protein knowledgebase in 2021. Nucleic Acids Res 2021;49(D1):D480–D489
16 Lai X, Wichers HJ, Soler-Lopez M, Dijkstra BW. Structure of human tyrosinase related protein 1 reveals a binuclear zinc active site important for melanogenesis. Angew Chem Int Ed Engl 2017;56 (33):9812–9815
17 Ismaya WT, Rozeboom HJ, Weijn A, et al. Crystal structure of Agaricus bisporus mushroom tyrosinase: identity of the tetramer subunits and interaction with tropolone. Biochemistry 2011;50 (24):5477–5486
18 Zhu D, Huang H, Pinkas DM, et al. 2-Amino-2,3-dihydro-1*H*-indene-5-carboxamide-based discoidin domain receptor 1 (DDR1) inhibitors: design, synthesis, and *in vivo* antipancreatic cancer efficacy. J Med Chem 2019;62(16):7431–7444
19 Zhang L, Zhang L, Guo Y, et al. MCDB: a comprehensive curated mitotic catastrophe database for retrieval, protein sequence alignment, and target prediction. Acta Pharm Sin B 2021;11 (10):3092–3104
20 Lipinski CA. Lead- and drug-like compounds: the rule-of-five revolution. Drug Discov Today Technol 2004;1(04):337–341
21 Fischer A, Smieško M, Sellner M, Lill MA. Decision making in structure-based drug discovery: visual inspection of docking results. J Med Chem 2021;64(05):2489–2500
22 Nazir Y, Saeed A, Rafiq M, et al. Hydroxyl substituted benzoic acid/cinnamic acid derivatives: tyrosinase inhibitory kinetics, anti-melanogenic activity and molecular docking studies. Bioorg Med Chem Lett 2020;30(01):126722
23 Swinney DC. Chapter 18 - Molecular mechanism of action (MMoA) in drug discovery. In: Macor JE, ed. Annual Reports in Medicinal Chemistry. Cambridge, MA: Academic Press; 2011:301–317
24 Cheng Y, Prusoff WH. Relationship between the inhibition constant (K1) and the concentration of inhibitor which causes 50 per cent inhibition (I50) of an enzymatic reaction. Biochem Pharmacol 1973;22(23):3099–3108
25 Hassan M, Ashraf Z, Abbas Q, Raza H, Seo SY. Exploration of novel human tyrosinase inhibitors by molecular modeling, docking and simulation studies. Interdiscip Sci 2018;10(01):68–80
26 Bienert S, Waterhouse A, de Beer TA, et al. The SWISS-MODEL Repository-new features and functionality. Nucleic Acids Res 2017;45(D1):D313–D319
27 Consortium TUUniProt Consortium. UniProt: the universal protein knowledgebase in 2021. Nucleic Acids Res 2021;49(D1): D480–D489
28 Kataria R, Khatkar A. Molecular docking, synthesis, kinetics study, structure-activity relationship and ADMET analysis of morin analogous as *Helicobacter pylori* urease inhibitors. BMC Chem 2019;13(01):45–45
29 Shivakumar D, Harder E, Damm W, Friesner RA, Sherman W. Improving the prediction of absolute solvation free energies using the next generation OPLS force field. J Chem Theory Comput 2012; 8(08):2553–2558
30 Wang J, Zhu Y, Chen J, et al. Identification of a novel PAK1 inhibitor to treat pancreatic cancer. Acta Pharm Sin B 2020;10(04): 603–614
31 Luo X, Zhao Y, Tang P, et al. Discovery of new small-molecule cyclin-dependent kinase 6 inhibitors through computational approaches. Mol Divers 2021;25(01):367–382
32 Adasme MF, Linnemann KL, Bolz SN, et al. PLIP 2021: expanding the scope of the protein-ligand interaction profiler to DNA and RNA. Nucleic Acids Res 2021;49(W1):W530–W534
33 Choi J, Choi KE, Park SJ, Kim SY, Jee JG. Ensemble-based virtual screening led to the discovery of new classes of potent tyrosinase inhibitors. J Chem Inf Model 2016;56(02):354–367
34 Mutahir S, Khan MA, Khan IU, et al. Organocatalyzed and mechanochemical solvent-free synthesis of novel and functionalized bis-biphenyl substituted thiazolidinones as potent tyrosinase inhibitors: SAR and molecular modeling studies. Eur J Med Chem 2017;134:406–414
35 Hu YH, Chen QX, Cui Y, et al. 4-Hydroxy cinnamic acid as mushroom preservation: anti-tyrosinase activity kinetics and application. Int J Biol Macromol 2016;86:489–495
36 Ullah S, Kang D, Lee S, et al. Synthesis of cinnamic amide derivatives and their anti-melanogenic effect in α-MSH-stimulated B16F10 melanoma cells. Eur J Med Chem 2019;161:78–92